EXPERIMENTAL STUDIES ON CONGO RED ADSORPTION BY TEA WASTE IN THE PRESENCE OF SILICA AND Fe_2O_3 NANOPARTICLES

Alireza Shojamoradi[1], Hossein Abolghasemi[1,2]*, Mohamad Esmaili[1], Mohammad Foroughi-dahr[1], and Hooman Fatoorehchi[1]

[1] Center for Separation Processes Modeling and Nano-Computations, School of Chemical Engineering, College of Engineering, University of Tehran, P.O. Box 11365-4563, Tehran, Iran

[2] Oil and Gas Center of Excellence, University of Tehran, Tehran, Iran

ABSTRACT

In this work, the adsorption of the anionic dye, Congo red (CR), from aqueous solution by using tea waste (TW) has been carried out at 30 °C. The equilibrium sorption isotherms and kinetics were investigated. The equilibrium adsorption was studied by the Langmuir and Freundlich models of adsorption. The experimental results manifested that the Langmuir isotherm was the best model for the adsorption of CR by TW and implied the monolayer adsorption of CR on TW with the adsorption capacity of 40.6 mg/g at 30 °C. The kinetic data resulted from batch experiments were analyzed using pseudo-first-order and pseudo-second-order models. It was found that pseudo-second-order model provided the best fit for the experimental data (R^2>0.99). The results illustrated that both silica and Fe_2O_3 nanoparticles increased the adsorption of CR on TW by about 5% and 10% at 30 °C, respectively. The results suggested that TW should be a potential low-cost adsorbent for the removal of CR from aqueous solution.

Keywords: Tea Waste, Congo red, Adsorption, Silica Nanoparticles, Fe_2O_3 Nanoparticles.

INTRODUCTION

The discharged effluents from dyeing industries are highly polluted with large amounts of pollutants such as dissolved and suspended solids [1,2]. The release of such effluents has a harmful influence on environment and aqueous systems. Moreover, the presence of even small amounts of dyes in water is highly visible [3,4]. Dyes are categorized into three main groups, namely (a) anionic: direct, acid, and reactive dyes; (b) cationic: basic dyes; and (c) nonionic: disperse dyes [5]. Congo red (CR) is a benzidine-based anionic diazo dye. It should be noted that the azo dyes are the commonest dyes used and account for 65-70% of the total dyes produced. Consequently, several treatment processes have been developed for the removal of dyes from aqueous solutions, including electrochemical degradation [6], solar photo-Fenton and biological processes [7], sonochemical degradation [8], oxidation or ozonation [9], and adsorption [10]. The adsorption process by activated carbon is the most effective process due to its

***Corresponding author**
Hossein Abolghasemi
Email: abolghasemi.ha@gmail.com
Tel: +98 21 6111 2186
Fax: +98 21-6695 4051

Article history
Received: April 7, 2013
Received in revised form: May 27, 2013
Accepted: May 28, 2013
Available online: October 25, 2013

simplicity despite of its run cost and regeneration difficulties [11]. Several investigations have been conducted in order to examine more economical adsorbent for the removal of dyes by adsorption processes. The research works show various alternatives such as jujuba seeds [12], banana peel [13], rice husk [14], chitosan [15], kaolin [16], and bentonite [17] as the adsorbent for the removal of CR from aqueous solutions.

Tea plants are commonly cultivated in the northern area of Iran. The tea waste (TW) has been used for the removal of many pollutants, including heavy metals and dyes from aqueous solution. Çay et al. used tea industry waste for the removal of copper and cadmium (II) from aqueous solutions with the adsorption capacity of 8.64 and 11.29 mg/g, respectively [18]. Malkoc et al. conducted experiments adsorbing hexavalent chromium (VI) onto tea waste with the maximum adsorption capacity of 54.65 mg/g [19]. Nasuha et al. employed rejected tea for the removal of methylene blue from aqueous solution with the adsorption capacity of 147.154 mg/g [20]. With the development of nanomaterial technology, nanoparticles have been attending much attention because of their application and effect in mass and heat transfer processes. Several works have been conducted to evaluate the heat transfer increase in the presence of nanoparticles [21,22]. Besides, many researchers have investigated the effect of adding nanoparticles to the liquid phase on the mass transfer. Sonneveld et al. investigated the effect of SiC on the mass transfer to a RDE system [23]. Veilleux and Coulome found larger dye diffusion in Al_2O_3 nanofluids [24]. The object of this study was to analyze the adsorption behavior of TW for the removal of CR from aqueous solution. The equilibrium and kinetic of the adsorption process were investigated using the isotherm and kinetic models. The characteristics of TW were investigated using FTIR, SEM, and BET analyses. Besides, the influence of silica and Fe_2O_3 nanoparticles has been studied.

EXPERIMENTAL

Chemicals

Congo red (CR), $C_{32}H_{22}N_6Na_2O_6S_2$, was supplied by Merck Company. Its C.I. No. is 22120, FW=696, and λ_{max}=495. The molecular structure of CR is illustrated in Figure 1. silica nanoparticles (surface area of 200 m^2/g, primary particle diameter of 12 nm, Degussa Company) and Fe_2O_3 nanoparticles (surface area of 60 m^2/g, primary particle diameter of 40 nm, Degussa Company) were used as the nanoparticles in this study.

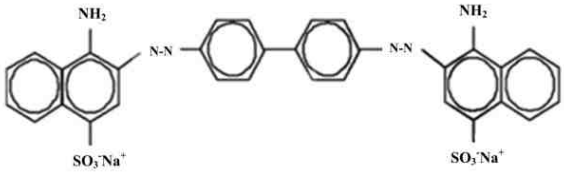

Figure 1: Molecular structure of CR

Preparation of the Adsorbent

The tea leaves used in this work were produced in tea plantations from the northern area of Iran. TW was collected and, prior to the experiments, it was boiled with water several times until the filtrated water was clear and completely colorless. TW was then washed with distillated water and was oven dried for 48 hrs at 70 °C. The sample was ground and sieved to obtain a particle size of 125-250 mm and stored in an airtight container for further use.

Preparation of Nanofluid Solution

For preparing the silica and Fe_2O_3 nanofluids, proper amounts of silica and Fe_2O_3 nanoparticles were added to distillated water, respectively and then dispersed in water, by using ultrasonication for about an hour (Misonix sonicator 3000). Morphological characteristics of silica and Fe_2O_3 are shown in Figures 2, and 3 respectively. According to these figures, the scanning elec-

tron microscopy (SEM) images illustrate the nanoparticles as spherical and nanoscale particles. Dynamic light scattering (DLS) images depict 56 and 62 nm as the mean diameter of silica and Fe_2O_3 particles, respectively.

(a)

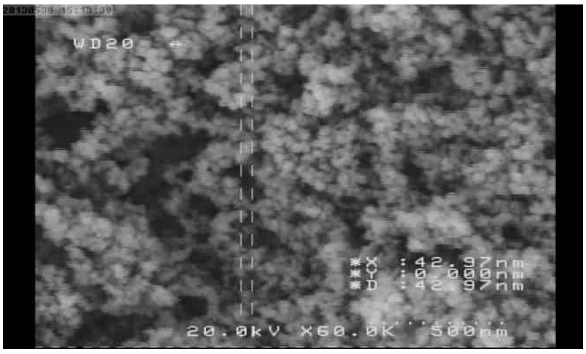

(b)

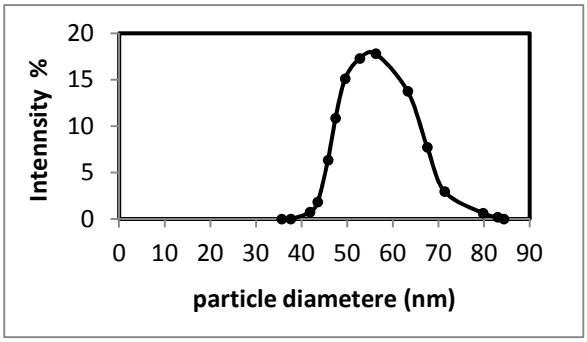

Figure 2: (a) SEM image of silica nanoparticles; (b) DLS image of silica nanofluid.

Batch Equilibrium and Kinetic Studies

Equilibrium experiments were carried out in 100 mL stoppered Erlenmeyer flasks by adding fixed amounts of adsorbent (0.7 g) in 50 mL of dye solution of different initial concentration (50-250 mg/L).

The agitation was provided for 12 hrs at a constant speed of 200 rpm at 30 °C in a thermostatic rotary shaker. The same procedure was performed in the presence of different amounts of nanoparticles (silica and Fe_2O_3) in CR solution (20-40 ppm). The CR concentrations were analyzed by a UV-vis spectrophotometer (UNICAM, 8700 series, USA) at the wavelength of maximum absorbance equal to 495 nm.

(a)

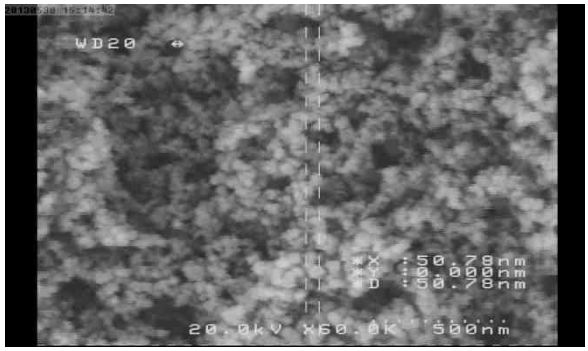

(b)

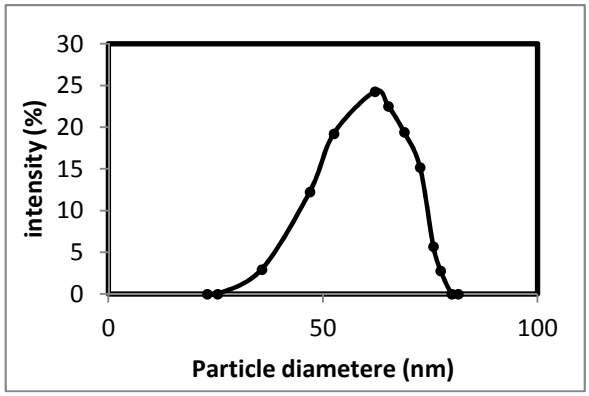

Figure 3: (a) SEM image of Fe_2O_3 nanoparticles; (b) DLS image of Fe_2O_3 nanofluid.

The dye removal percentage of adsorption is calculated as given below:

$$\text{Removal Percentage} = \frac{(C_0 - C_e)}{C_0} \times 100 \qquad (1)$$

where, C_0 and C_e (mg/L) denote the liquid phase concentration of dye at initial time and the equilibrium concentration in solution respectively. In the kinetic part, these samples were withdrawn at preset time intervals. The amount of CR adsorbed at time t, q_t (mg/g), was calculated based on the following mass balance relationship:

$$q_t = \frac{(C_0 - C_t)V}{W} \qquad (2)$$

where, C_t (mg/L) is the liquid phase concentration of dye at time t; V stands for the volume of the solution (L) and W is the mass of the dry adsorbent used (g).

RESULTS AND DISCUSSION

Adsorption Kinetic

The effects of contact time and initial concentration on the adsorption of CR are depicted in Figure 4. According to Figure 4, an increase in the initial dye concentration results in a rise in the adsorption of CR on TW. The adsorption uptake was rapid for the first stages of the adsorption; then the adsorption rate decreased and finally reached a saturation level. The equilibrium states were achieved at about 150 min for the initial concentration less than 150 mg/L and at 350 min for an initial concentration of 200 and 250 mg/L. Higher initial concentrations provide more important driving force to overcome the mass transfer resistance between the solid (TW) and aqueous phases (CR solution). Hence the equilibrium adsorption increased from 3.11 to 15.19 mg/g as the initial concentration of CR was increased from 50 to 250 mg/L. The equilibrium times of 200 min, 2.5 hrs, and 6 hrs were reported for the adsorption of CR on broad been peels [25], cattail root [26], and jajuba seeds [12] respectively.

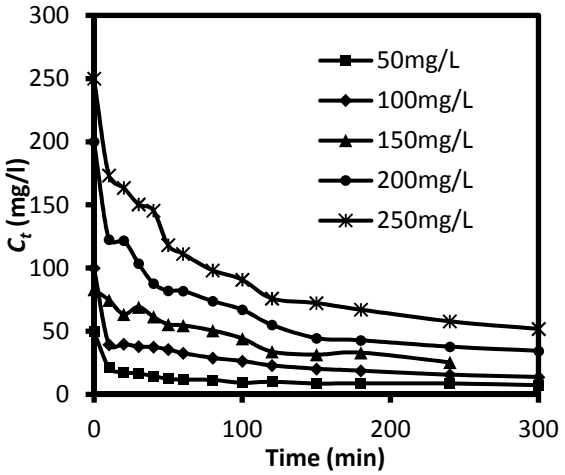

Figure 4: The adsorption of CR onto TW for different initial concentrations; (*T* = 30 °C, agitation rate= 200 rpm, volume=50 ml, and W= 0.7 g).

Isotherm Studies

The Freundlich and Langmuir models are the commonest isotherm models used to evaluate the relationship between the equilibrium concentration on the adsorbent and in the solution. The Freundlich isotherm is an empirical model based on the assumption of the heterogeneous surfaces with a non-uniform adsorption heat distribution over the surface of the adsorbent. The Freundlich isotherm is presented as:

$$q_e = K_f C_e^{1/n} \quad (3)$$

where, K_f is the adsorption constant and n is the constant describing the adsorption intensity. Values of n>1 show a favorable adsorption process [3,27]. The values of K_f, n, and the correlation coefficient obtained for the Freundlich model are summarized in Table1. The value of n is 1.437 indicating the favorable adsorption. The Langmuir isotherm model assumes monolayer adsorption onto a homogenous surface [28,3]. The Langmuir isotherm is expressed as:

$$q_e = \frac{q_m b C_e}{1 + b C_e} \quad (4)$$

where, q_m (mg/g) is the maximum adsorption capacity of TW and b (L/mg) is the Langmuir isotherm constant. The values of R^2 and Langmuir constants are given in Table 1.

The dimensionless constant, R_L, is taken to express the favorability of the adsorption and is calculated as:

$$R_L = \frac{1}{(1 + b C_0)} \quad (5)$$

The amounts of $0<R_L<1$ indicate a favorable adsorption [3]. The values of R_L for the adsorption of CR onto TW are shown in Figure 5. According to Figure 5, the R_L values are in the range of 0.14-0.45 which implies that the adsorption of CR onto TW is a favorable process. Increasing the initial concentration, the adsorption approaches toward the irreversibility.

Table 1: Isotherm constant parameters and the correlation coefficients for the adsorption of CR onto TW and vibratory mill treated TW at 30°C

Isotherm	Isotherm constants
Freundlich	K_f=1.299 (mg/g(L/mg)$^{1/n}$), n=1.437, R^2=0.9973
Langmuir	q_m=32.9(mg/g), b=0.02449 (L/mg), R^2=0.9996

The experimental equilibrium data and the predicted data based on the aforementioned isotherm models for the adsorption of CR on TW are illustrated in Figure 6. It can be seen from Figure 6 that both of the isotherm models provide good fit for the experimental data. However, the Langmuir isotherm exhibited a better fit compared to the Freundlich model.

According to Table 1, the R^2 value of the Langmuir is higher than that of the Freundlich isotherm, although both of the isotherm models have high R^2 values. Therefore, the adsorption of CR on TW takes place on a homogenous surface as a monolayer adsorption.

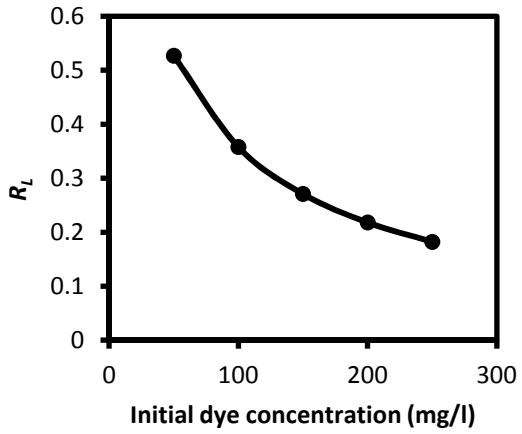

Figure 5: The separation factor for the adsorption of CR on TW at 30 °C

The maximum adsorption capacity (q_m) for the removal of CR onto TW is presented in Table 2. Besides, the adsorption capacities of several adsorbents for the removal of CR are shown in this Table. In comparison with the other adsorbents, TW has a relatively large adsorption capacity for the removal of CR.

Table 2: Adsorption capacity of CR on different adsorbents

Adsorbent	q_m (mg/g)	References
Neem leaf	41.2-28.3	[29]
Jajuba seads	55.56	[12]
Cattail root	38.79	[26]
Tea waste	32.9	Present work
Raw pine cone	19.18	[10]
Bagasse fly ash	11.89	[30]
Banana peel	11.2	[13]
Pomegranate	10	[31]
Kaoline (Ceram)	7.27	[16]
Acid activated red mud	4.05	[32]

The pseudo-first-order kinetic models do not provide a good fit for the experimental data, which indicates that this model cannot satisfactorily evaluate the kinetics of the adsorption. It is depicted in Figure 7 that pseudo-second-order model provides a straight line for all the initial concentrations. The values of q_{ecal} of the pseudo-second-order model agree with the q_{eexp}. The high values of the corresponding coefficient of the pseudo-second-order model also affirm the goodness of the fit.

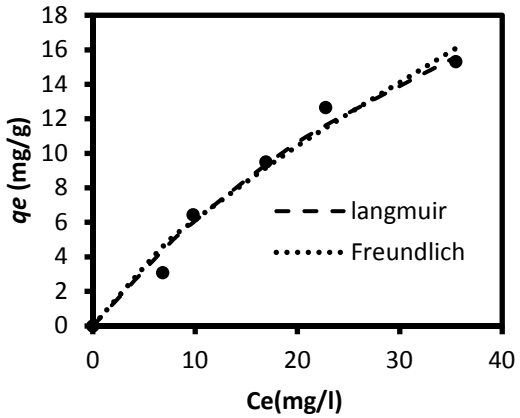

Figure 6: Isotherm plots for CR removal on TW at 30 °C.

Kinetic Modeling

The kinetic behavior of the adsorption of CR on TW was studied using a Lagergren pseudo-first-order model and a pseudo-second-order model.

The pseudo-first-order model defines the kinetics of the adsorption as reads:

$$\log(q_e - q_t) = \log q_e - \left(\frac{k_1}{2.303}\right)t, \quad (6)$$

where, k_1 (1/min) is the rate constant of pseudo-first-order adsorption. The values of k_1 and q_e can be evaluated from the plots of $\log(q_e-q_t)$ versus time [33,34]. The values of k_1, q_e, and the corresponding coefficients are listed in Table 3.

The pseudo-second-order equation is expressed by the following equation:

$$\frac{t}{q_t} = \frac{1}{k_2 q_e^2} + \frac{t}{q_e}, \quad (7)$$

where, k_2 (g/mg.min) is the constant of pseudo-second-order adsorption. Plotting t/q_t versus t gives the amounts of k_2 and q_e (Figure 7) [35]. The values of k_2, q_e, and R^2 are presented in Table 3.

The R^2 values obtained for the pseudo-second-order model are close to the unity. A similar result was reported for the adsorption of CR from an aqueous solution over the jujube seed [12] and raw pine [10].

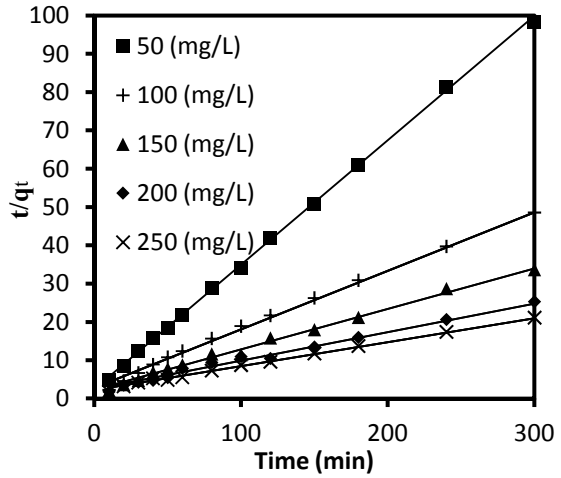

Figure 7: The fitting of pseudo-second-order model for the adsorption of CR onto TW at different initial concentrations

The Influence of Nanoparticles

Figures 8 and 9 illustrate the effect of the presence of nanoparticles of Fe_2O_3 and silica in the adsorption process of CR onto TW. Silica nanoparticles at the concentration of 20 ppm caused the adsorption of CR to increase by about 5%; additionally, Fe_2O_3 nanoparticles at the concentration of 20 ppm caused the adsorption of CR to rise by about 10% (Figures 8 and 9). It is also obvious from Figures 8 and 9 that the increase of the nanoparticle concentration has no significant effect on the adsorption of CR. The increase of the adsorption uptake in the presence of the nanoparticles can be ascribed to the mass transfer enhancements and the increase of mass diffusivity. The mass transfer enhancements of dyes have been reported by many researchers [24]. Besides, Brownian motion is an important mechanism applied to interpret the adsorption enhancement. It can be concluded that the Brownian motion of nanoparticles can create micro/nano scale convection to increase mass transfer of dye molecules. Accordingly, the adsorption of dyes on the adsorbent surface can be impressed by this phenomenon [24,36]. Moreover, the presence of nanoparticles may decrease the boundary layer thickness over the adsorbent particles, which leads to an increase in the diffusion rate of CR particles inside the adsorbent pores.

Characterization of TW

Fourier transform infrared (FTIR) analysis of TW before and after CR adsorption were studied in the range of 400-4000 cm^{-1} to determine the surface functional groups (Figure 10). The spectra were achieved using an FTIR spectro-photometer (Bruker Tensor, 27, Germany). The functional groups on the surface of the adsorbent provide active sites for the adsorption of CR. According to Figure 10, several peaks can be observed indicating that TW is composed of various functional groups.

Table 3: Adsorption kinetic parameters for pseudo-first-order and pseudo-second-order models of the adsorption of CR on TW

Initial concentration (mg/l)	$q_{e,exp}$ (mg/g)	Pseudo-first-order kinetic model			Pseudo-first-order kinetic model		
		k_1 (1/min)	$q_{e,cal}$ (mg/g)	R^2	k_2(g/mg min) 10^3	$q_{e,cal}$ (mg/g)	R^2
50	3.111	0.0087	0.2549	0.565	43.77	3.077	0.999
100	6.453	0.0129	6.2359	0.863	8.39	6.579	0.999
150	9.229	0.0154	20.9846	0.809	4.90	9.524	0.999
200	13.137	0.0111	69.4544	0.911	2.25	13.514	0.999
250	15.192	0.0187	184.6716	0.978	1.59	16.00	0.999

Spectra bands observed at 3417 cm^{-1} is attributed to the O-H stretching vibrations due to inter and intra molecular hydrogen bonding of polymeric compounds such as alcohols, phenols, and carboxylic acids as in pectin, cellulose, and lignin. Therefore, it can be concluded that the free hydroxyl groups are present on the adsorbent surface [10,37].

The peaks at 2923 and 2858 cm^{-1} are ascribed to the aliphatic C-H group. The peaks at 2356 and 1631 cm^{-1} are assigned to C=N and C=O stretching vibrations, respectively. The peak at 1552 cm^{-1} is attributed to secondary amine groups. The peaks at 1456 and 1388 cm^{-1} are both related to the symmetric bending of CH_3. The peaks at 1249, 1049, 617, and 473 cm^{-1} correspond to stretching vibration of SO_3, C=O, -C-C-, and amine groups, respectively [10,37]. Figure 10 shows that some peaks are shifted or disappeared after the adsorption process. It can be seen that the peak at 473 cm^{-1} is disappeared. Besides, it should be noted that some remarkable changes can be seen after the adsorption of CR. According to Figure 10, there is considerable difference in the intensity of the band C=O, -C-C-, amine group, and SO_3 group, which implies that CR binding occurs at the aforesaid functional groups. IR adsorption bands and corresponding possible functional groups for TW before and after the adsorption are presented in Table 4.

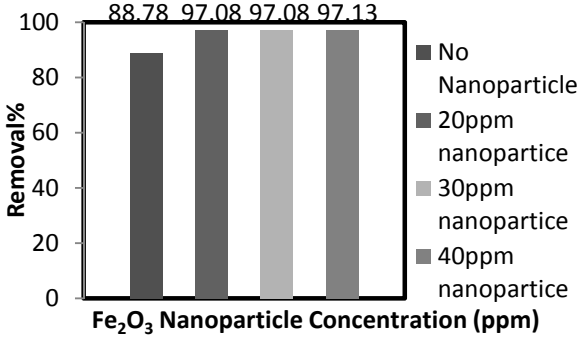

Figure 8: The effect of Fe_2O_3 nanoparticles on the adsorption of CR on TW at 30 °C

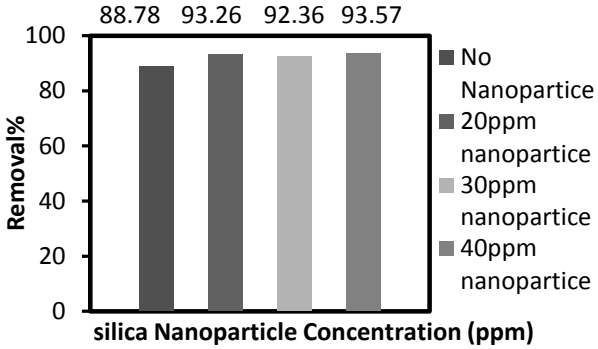

Figure 9: The effect of silica nanoparticles on the adsorption of CR on TW at 30 °C

The surface morphology of TW was analyzed by scanning electronic microscopy (SEM) before and after CR adsorption (Figures 11 and 12). It is clear from Figure 12 that TW has highly heterogeneous pores within its particles, which is suitable for adsorption processes.

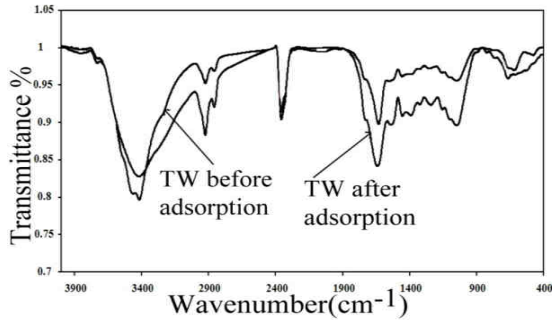

Figure 10: FTIR spectra of TW before and after adsorption

This figure also reveals a meaningful change in the structure of TW after the adsorption of CR. The BET surface area, total pore volume, and average pore size of TW were measured to be 4.6 m^2/g, 0.0052 cm^3/g, and 47 Å respectively using a ChemBET 3000 Quantachrome instrument.

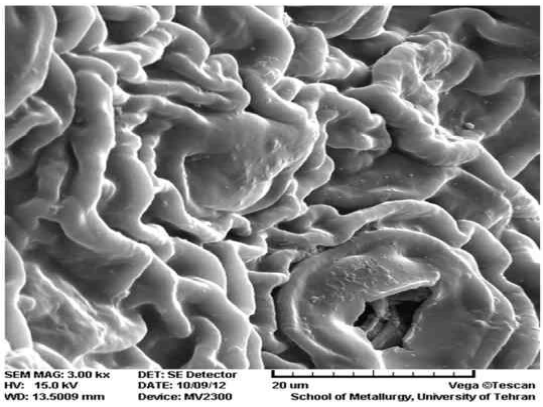

Figure 11: SEM images of the original TW

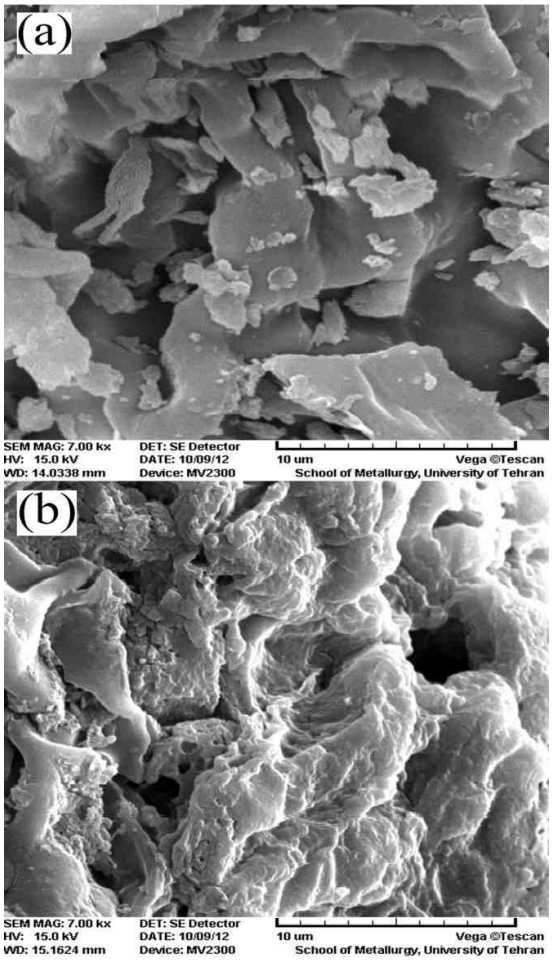

Figure 12: SEM images of TW: (a) before adsorption; (b) after adsorption

Table 4: FTIR of TW before and after adsorption

IR peak	Frequency (cm^{-1})			Assignment
	Before adsorption	After adsorption	Differences	
1	3417.69	3417.69	0	Bonded –OH groups
2	2923.94	2925.87	+1.93	Aliphatic –C–H group
3	2858.36	2858.36	0	Aliphatic –C–H group
4	2356.89	2358.88	+1.99	-C=N strertching
5	1631.70	1639.41	+7.71	–C=O stretching
6	1552.62	1542.98	-9.64	Secondary amine group
7	1456.18	1454.25	-1.93	Symmetric bending of CH_3
8	1388.68	1390.61	+1.93	Symmetric bending of CH_3
9	1249.81	1242.10	-7.71	$–SO_3$ stretching
10	1049.22	1045.37	-3.85	C=O stretching
11	617.19	663.48	+46.29	–C–C– group
12	478.32	disappeared	unknown	Amine group

CONCLUSIONS

The present study shows that TW is an effective adsorbent for the adsorption of CR from aqueous solutions. Adsorption process follows the Langmuir isotherm models with a maximum adsorption capacity of 40.6 mg/g. The pseudo-second-order model can be used to predict the kinetics of the adsorption. It is also found that the presence of nanoparticles (silica and Fe_2O_3) enhances the adsorption of CR on TW by about 5% and 10% respectively.

REFERENCES

[1] Mittal, A., Mittal, I., Malviya, A., Gupta, V. K. "Adsorptive Removal of Hazardous Anionic Dye Congo Red from Wastewater Using Waste Materials and Recovery by Desorption," *J. Colloid Interface Sci*., **2009**, *340*, 16-26.

[2] Ozcan, A. S. and Ozcan, A. "Adsorption of Acid Dyes from Aqueous Solutions onto Acid-activated Bentonite," *J. Colloid Interf. Sci*., **2004**, *276*, 39–46.

[3] Hameed, B.H. "Spent Tea Leaves: A New Non-conventional and Low-cost Adsorbent for Removal of Basic Dye from Aqueous Solution," *J. Hazard. Mater*., **2009**, *161*, 753-759.

[4] Rafatullah, M., Sulaiman, O., Hashim, R., Ahmad, A. "Adsorption of Methylene Blue on Low-cost Adsorbents: A Review," *J. Hazard. Mater*., *2010*, *177*, 70-80.

[5] Gupta, V. K., Suhas "Application of Low-cost Adsorbents for Dye Removal: A Review," *J. Environ. Manage*., **2009**, *90*, 2313-2342.

[6] Fan, L., Zhou, T., Yang, W., Chen, G., Yang, F. "Electrochemical Degradation of Aqueous Solution of Amaranth Azo Dye on ACF under Potentiostatic Model," *Dyes Pigments*, **2008**, *76*, 440-446.

[7] Garcıa-Montano, J., Perez-Estrada, L., Oller, I., Maldonado, M. I., Torrades, F., Peral, J. "Pilot Plant Scale Reactive Dyes Degradation by Solar Photo-Fenton and Biological Processes," *J. Photochem. Photobiol. A*, **2008**, *195*, 205-214.

[8] Abbasi, M., Asl, N. R. "Sonochemical Degradation of Basic Blue 41 Dye Assisted by Nano TiO_2 and H_2O_2," *J. Hazard. Mater*, **2008**, *153*, 942-947.

[9] Reynolds, G., Graham, N., Perry, R., Rice, R. G. "Aqueous Ozonation of Pesticides: A Review," *Ozone Sci. Eng*., **1989**, *11*, 339-382.

[10] Dawood, S., Sen, T. K. "Removal of Anionic Dye Congo Red from Aqueous Solution by Raw Pine and Acid-treated Pine Cone Powder as Adsorbent: Equilibrium, Thermodynamic, Kinetics, Mechanism, and Process Design," *Water Res*., **2012**, *46*, 1933-1945.

[11] Gong, R., Ding, Y., Li, M., Yang, C., Liu, H., Sun, Y "Utilization of Powdered Peanut Hull as Biosorbent for Removal of Anionic Dyes from Aqueous Solution," *Dyes Pigments*, **2005**, *64*, 187-192.

[12] Somasekhara Reddy, M. C., Sivaramkrishna, L., Varada Reddy, A. "The Use of an Agricultural Waste Material, Jujuba Seeds for the Removal of Anionic Dye (Congo Red) from Aqueous Medium," *J. Hazard. Mater*., **2012**, *203*, 118-127.

[13] Annadurai, G., Juang, R. S., Lee, D. J. "Use of Cellulose-based Wastes for Adsorption of Dyes from Aqueous Solutions," *J. Hazard. Mater*, **2002**, *92*, 263-274.

[14] Wang, S., Boyjoo, Y., Choueib, A., Zhu, Z. H. "Removal of Dyes from Aqueous Solution Using Fly Ash and Red Mud," *Water Res*., **2005**, *39*, 129-138.

[15] Wang, L., Wang, A "Adsorption Characteristics of Congo Red onto the Chitosan/Montmorillonite Nanocomposite," *J. Hazard. Mater*, **2007**, *147*, 979-985.

[16] Vimonses, V., Lei, S., Jin, B., Chow, C. W. K., Saint, C. "Adsorption of Congo Red by Three Australian Kaolins," *Appl. Clay Sci*., **2009**, *43*, 465-472.

[17] Bulut, E., Özacar, M., Ayhan Şengil, İ. "Equilibrium and Kinetic Data and Process Design for Adsorption of Congo Red onto Bentonite," *J. Hazard. Mater.,* **2008**, *154*, 613-622.

[18] Çay, S., Uyanık, A., Öza¸sık, A. "Single and Binary Component Adsorption of Copper(II) and Cadmium(II) from Aqueous Solutions Using Tea-industry Waste," *Sep. Purif. Technol*., **2004**, *38*, 273-280.

[19] Malkoc, E., Nuhoglu, Y., "Potential of Tea Factory Waste for Chromium (VI) Removal from Aqueous Solutions: Thermodynamic and Kinetic Studies," *Sep. Purif. Technol*., **2007**, *54*, 291-298.

[20] Nasuha, N., Hameed, B.H., Mohd Din, A.T. "Rejected Tea as a Potential Low-cost Adsorbent for the Removal of Methylene Blue," *J. Hazard. Mater.,* **2010**, *175*, 126-132.

[21] Keblinski, P., Phillpot, S.R., Choi, S.U.S., Eastman, J.A. "Mechanism of Heat Flow in Suspensions of Nanosized Particles (Nanofluid)," *Int. J. Heat Maass Tran*., **2002**, *45*, 855–863.

[22] Prasher, R., Phelan, P. E., Bhattacharya, P."Effect of Aggregation Kinetics on the Thermal Conductivity of Nanoscale Colloidal Solutions (Nanofluid)," *Nanoletters*, **2006**, *6*, 1529-1534.

[23] Sonneveld, P. J., Visscher, W., Barendrecht, E. "The Influence of Suspended Particles on the Mass Transfer at a Rotating Disc Electrode: Non-conducting Particles," *J. Appl. Electrochem*., **1990**, *20*, 563-574.

[24] Veilleux, J., Coulombe, S. "A Total Internal Reflection Fluorescence Microscopy Study of Mass Diffusion Enhancement in Water-based Alumina Nanofluids," *J. Appl. Phys*., **2010**, *108*, 104316-104318.

[25] Hameed, B. H., El-Khaiary, M. I., "Sorption Kinetics and Isotherm Studies of a Cationic Dye Using Agricultural Waste," *J. Hazard. Mater*., **2008**, *154*, 639-648.

[26] Hu, Z., Chen, H., Ji, F., Yuan, S. "Removal of Congo Red from Aqueous Solution by Cattail Root," *J. Hazard. Mate.,* **2010**, *173*, 292-297.

[27] Freundlich, H. "Über die Adsorption in lösungen (Adsorption in solution)," *C. Phys. Chem*., **1906**, *57*, 384-470.

[28] Langmuir, I. "The Adsorpeion of Gases on Plane Surfaces of Glass, Mica and Platinum," *J. Am. Chem. Soc*., **1918**, *40*, 1361-1403.

[29] Bhattacharyya, K. G., Sharma, A., "Azadirachta Indica Leaf Powder as an Effective Biosorbent for Dyes: a Case Study with Aqueous Congo Red Solutions," *J. Environ. Manage*., **2004**, *71*, 217-229.

[30] Mall, I. D., Srivastava, V. C., Agarwal, N. K., Mishra, I. M. "Removal of Congo red from Aqueous Solution by Bagasse Fly Ash and Activated Carbon: Kinetic Study and Equilibrium Isotherm Analyses," *Chemosphere*, **2005**, *61*, 492-501.

[31] Ghaedi, M., Tavallali, H., Sharifi, M., Nasiri-Kokhdan, S., Asghari, A. "Preparation of Low-cost Activated Carbon from Myrtus Communis and Pomegranate and their Efficient Application for Removal of Congo Red from Aqueous Solution," *Spectrochim Acta Pt. A-mol. Bio.,* **2012**, *86*, 107-114.

[32] Tor, A., Gengeloglu, Y. "Removal of Congo Red from Aqueous Solution by Adsorption onto Acid-activated Red Mud," *J. Hazard. Mater*., **2006**, 138, 409-415.

[33] Lagergren, S. "About the Theory of So-called Adsorption of Soluble Substances," *K. Sven. Vetenskapsakad. Handl*., **1898**, *24*, 1-39.

[34] Ho, Y. S. "Citation Review of Lagergren Kinetic Rate Equation Adsorption Reactions, Scientometrics," **2004**, *59*, 171-177.

[35] Ho, Y. S., Mc Kay, G. "Pseudo-second Order Model for Sorption Processes," *Process Biochem*., **1999**, *34*, 451-465.

[36] Feng, X., Johnson, D. W. "Mass Transfer in SiO_2 Nanofluids: A Case against Purported Nanoparticle Convection Effects," *Int. J. Heat Mass Transfer*, **2012**, *55*, 3447-3453.